



HAL
open science

Micro-bubble encapsulation by electrostatic templating with ionic surfactants

Vance Bergeron, Ramon Planet, Stéphane Santucci

► **To cite this version:**

Vance Bergeron, Ramon Planet, Stéphane Santucci. Micro-bubble encapsulation by electrostatic templating with ionic surfactants. *Physical Review Applied*, 2022, 10.1103/PhysRevApplied.18.L011001 . hal-03806349

HAL Id: hal-03806349

<https://hal.science/hal-03806349>

Submitted on 7 Oct 2022

HAL is a multi-disciplinary open access archive for the deposit and dissemination of scientific research documents, whether they are published or not. The documents may come from teaching and research institutions in France or abroad, or from public or private research centers.

L'archive ouverte pluridisciplinaire **HAL**, est destinée au dépôt et à la diffusion de documents scientifiques de niveau recherche, publiés ou non, émanant des établissements d'enseignement et de recherche français ou étrangers, des laboratoires publics ou privés.

Micro-bubble encapsulation by electrostatic templating with ionic surfactants

Vance Bergeron, Ramon Planet, and Stéphane Santucci

Université Lyon, ENS de Lyon, CNRS, Laboratoire de Physique, Lyon F-69342, France

We propose an original micro-bubble encapsulation process, using electrostatics as a driving force to guide either particles or polymerizable precursors to the bubble surface. Taking advantage of attractive interactions between surfactant-laden charged bubbles and oppositely charged self-assembling species, our method produces capsules with diverse protective shells that remain stable for years. Considering heterogeneous electrostatic double-layer interactions, we quantitatively predict critical particle surface potentials required for complete encapsulation. The particle-based shells can be disintegrated with a pH adjustment, allowing for a controlled release of encapsulated payloads, while the glassy continuous silicate capsules are chemically resistant to pH changes. Our process which can be equally applied to liquid droplets easily scales up for industrial developments.

Micro-bubbles display unique properties allowing the design of functional fluids relevant for many industrial processes [1] for ultrasound imaging [2], drug delivery [3], wastewater treatment [4], cosmetic creams and food products [5–7]. However, they are intrinsically unstable: the pressure inside a micro-bubble follows Laplace’s law, which drives Ostwald ripening. Consequently, micro-bubbles are short lived, typically lasting for only a matter of minutes, which severely limits their use [8].

To extend their lifetime, micro-bubbles can be encapsulated, to prevent the release of their content, while also providing elastic properties to their interface. Lipid, protein layers, or cross-linking organic polymers are commonly used but they produce soft non-durable shells that deflate over time [9, 10]. Supramolecular architectures can encase emulsion drops and colloids, which upon removal of the internal phase create microcapsules [11–13]. Ultrasonic cavitation could also produce hollow mesoporous silica vesicles [14]. However, all of these methods do not generate long-lasting pressurized gas bubbles.

Originally exploited in flotation processes [15], and later reported by Ramsden [16] and Pickering [17], colloids attached to bubbles and oil drops have been observed to stabilize foams and emulsions [18–20]; a practice used in food and flotation industries for decades [21]. A factor contributing to particle adhesion and the subsequent dispersion stability is the particles’ hydrophobicity characterized by their three-phase contact angle [22]. When around 90° , energy balances establish that particle detachment from a gas-water interface is orders of magnitude higher than $k_B T$ [23]. However, limited complex chemical modifications of the colloids’ surfaces are needed to adjust their wettability, which can be easily altered during post-processing. Furthermore, pre-dispersing hydrophobic particles for use in aqueous solutions requires also multiple steps and a high level of energy. Consequently, a viable protocol for large-scale production and post-processing has yet to be developed.

More importantly, from a fundamental perspective, the hydrophobic particle interaction with the dispersed phase before attachment is still not clearly understood. The existence of a yet to be elucidated “hydrophobic force” to breach the thin-liquid-film that separates the particle

from the dispersed phase interface is still debated [24, 25]. While, recent advances in the measurement of a so-called “hydrophobic force” between bubble and particle have been obtained [25], a theoretical derivation from meaningful molecular parameters is still lacking. This ambiguity remains a central problem to a clear understanding of dispersions stabilized by hydrophobic particles.

Therefore, we propose in this Letter an original encapsulation process, using electrostatics interactions to drive either particles or polymerizable precursors to the bubble surface, and create a self-assembled encapsulating shell. Our general and simple approach can be quantitatively described by Derjaguin, Landau, Verveij, and Overbeek (DLVO) theory [26], considering heterogeneous electrostatic double-layer interactions [27]. Thus, it clarifies and circumvents the inherent difficulties and ambiguities of the so-called “Pickering” stabilization, allowing us to go beyond, by creating, at low cost and at industrial levels, a wide variety of novel objects, “*bubbloons & droploids*”, thanks to diverse protective shells, that strikingly remain stable for years. Furthermore, the particle-based capsules can be opened-up with a pH adjustment, while using silicate anions as encapsulating species, the subsequent glassy continuous silicate shells are chemically resistant, and the encapsulation is irreversible.

The basis of our encapsulation process resides in the use of ionic surfactants that adsorb to the gas-liquid interface of the micro-bubbles, providing a residual charge to the bubble surface, so that oppositely charged species will be attracted to it. We first show in the following that DLVO theory [26] can explain and predict quantitatively when particle adhesion to an ionic surfactant-saturated bubble surface and thus, encapsulation occurs: the total potential energy of interaction V_T between a bubble and a particle in solution is given by the sum of their Van der Waals, $V_d = -A_{132} \frac{R_1 R_2}{6h(R_1 + R_2)}$, and dissimilar electrical double layer interaction [27], $V_e = \frac{\epsilon_o \epsilon (\psi_1^2 + \psi_2^2) R_1 R_2}{4(R_1 + R_2)} \left[\frac{2\psi_1 \psi_2}{\psi_1^2 + \psi_2^2} \ln \left(\frac{1 + e^{-\kappa h}}{1 - e^{-\kappa h}} \right) + \ln(1 - e^{-2\kappa h}) \right]$, with R_1 , R_2 the bubble and particle radius, $\epsilon_o \epsilon$ the medium dielectric constant, ψ_1 and ψ_2 the surface potential of the bubble and particle, h the bubble-particle distance, A_{132} the composite Hamaker constant, and $1/\kappa$ the Debye length. Since $R_1 \gg R_2$, the interaction

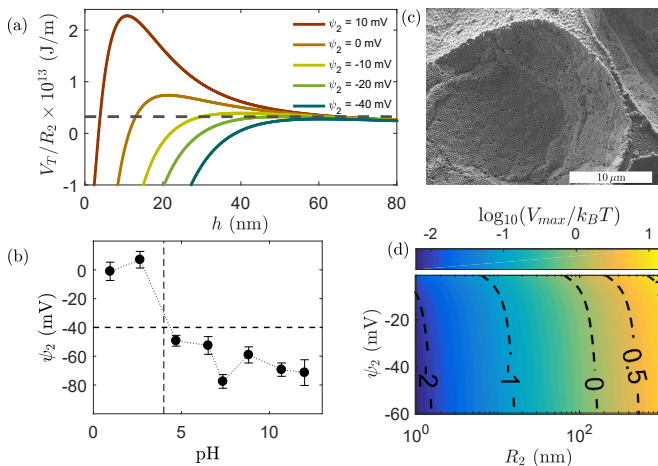


FIG. 1. (a) Bubble-particle interaction potential rescaled by the particle radius V_T/R_2 as a function of the distance h between the particle and the bubble surface, for the typical case of an air bubble dispersed in a solution of cationic surfactant, (bubble surface potential $\psi_1 \simeq +100\text{mV}$), for various surface potentials ψ_2 of spherical silica particle of radius $R_2 = 125\text{nm}$. The dashed line gives the value $k_B T/R_2$, at room temperature. (b) pH evolution of the surface potential of mono-disperse silica particles of radius $R_2 = 125\text{nm}$. A successful encapsulation was observed when the solution pH was larger than 4, corresponding to a zeta potential ψ_2 lower than -40mV . (c) A typical cryo-SEM image of such capsule. (d) 2D map of the energy barrier amplitude, renormalized by $k_B T$, in a logarithmic scale, $\log_{10}(V_{\max}/k_B T)$ as a function of the radius of the silica spheres R_2 , and their zeta potential ψ_2 . The dashed curves give various isolines.

potential $V_T = V_e + V_d$ can be simplified,

$$\frac{V_T}{R_2} \simeq \frac{\epsilon_0 \epsilon (\psi_1^2 + \psi_2^2)}{4} \times \left[\frac{2\psi_1 \psi_2}{\psi_1^2 + \psi_2^2} \ln \left(\frac{1 + e^{-\kappa h}}{1 - e^{-\kappa h}} \right) + \ln(1 - e^{-2\kappa h}) \right] - \frac{A_{132}}{6h}.$$

We consider a well characterized “ideal” case: a $100\ \mu\text{m}$ diameter air bubble in a cationic surfactant solution, such as Hexadecyl Trimethyl Ammonium Chloride (HTAC), at the critical micellar concentration, CMC $\simeq 10^{-3}\text{M}$, leading to a Debye length of $10\ \text{nm}$ [26], and a surface potential of $\psi_1 \simeq +100\ \text{mV}$ [28], interacting with mono-disperse silica spheres of $R_2 = 125\ \text{nm}$ radii. A composite Hamaker constant $A_{132} = -1 \times 10^{-20}\ \text{J}$ gives the repulsive Van der Waals forces for the silica-water-air thin-liquid-film between the particles and bubble [29]. On the other hand, the particle surface potential depends on the pH of the solution. Using a ZetaPALS instrument, we measured how the surface potential of such silica particles evolves with the solution pH, as shown in Fig.1(b). Successful bubble encapsulation occurred when the pH of the solution was larger than 4, corresponding to a drop in the particle surface potential lower than $-40\ \text{mV}$. A cryo-SEM image (Fig.1(c)) provides a typical example of such encapsulated micro-bubble. In these conditions,

the bubble-particle double-layer forces are sufficiently attractive to overcome Van der Waals repulsion, decreasing the corresponding energy barrier to a value comparable to $k_B T$, as shown in Fig.1(a); the particles will then spontaneously adhere to the bubble surface and subsequently encapsulate the bubble. This prediction for a critical particle surface potential is in excellent quantitative agreement with our experimental observations of bubble encapsulation and zeta potential measurements, without any adjustable parameters, which is, remarkably, often not the case when attempts are made to use DLVO theory [30]. Interestingly, it also corresponds to experimental results reported in particle flotation studies [31].

The potential energy V_T is directly proportional to the particles size R_2 . Thus, the smaller the particles, the lower the energy barrier. We display in Fig.1(d), a 2D map showing how this energy barrier (computed as the maximum value V_{\max} of V_T) evolves with both R_2 and the surface potential ψ_2 , for this ideal test case of monodisperse silica spheres, interacting with a cationic surfactant saturated air bubble. Such a map gives the typical range, in terms of size and zeta potential of the particles used (R_2, ψ_2), for a successful encapsulation, depending also on the energy level one can provide. The isoline $V_{\max} = k_B T$ shows when the energy barrier is equal to Boltzmann thermal energy fluctuations. Up until this value, the particles will spontaneously adhere to the bubble surface; Interestingly, for particles smaller than $50\ \text{nm}$, this barrier is always smaller than $k_B T$, even for low absolute value of their surface potential ψ_2 , which can explain the ubiquitous observation of bubbles and droplets stabilization with colloids. The encapsulation can also be facilitated by a more vigorous mixing, which could be required to encapsulate micro-bubbles with larger particles (up to a few μm for instance) and/or particles with a lower absolute zeta potential value.

To demonstrate the robustness of our novel encapsulation method, we have performed experiments with a variety of particles of different shapes (spheres, rods, needles, platelets), bulk materials (silica, boehmite, nacre), and either cationic (HTAC), or anionic (Lauroyl Sarcosinate (LS)) surfactant solutions at the CMC. Typical examples are shown Figs. 1 and 2. The bottom panel of Fig. 2 provides global macroscopic measurements of the volume of encapsulated micro-bubbles dispersions (typically around $25\ \text{mL}$), arbitrarily chosen after 10 days, V_{10} , normalized by their initial volume (measured right after their formulation), V_0 , as a function of the pH of the solution used. The bubbles were encapsulated either by silica spheres of around $100\ \text{nm}$ (left panel), silica rods of approximately $100\ \text{nm}$ long and $10\ \text{nm}$ large (middle panel), and nacre platelets of few microns (right panel). The corresponding pH evolution of their zeta potential ψ_2 is also displayed. The top panel of this figure, giving the volume of the stable encapsulated micro-bubbles dispersions V_{10}/V_0 as a function of the zeta potential of the encapsulating particles, multiplied by the polarity of the ionic surfactant head group, rationalizes our various

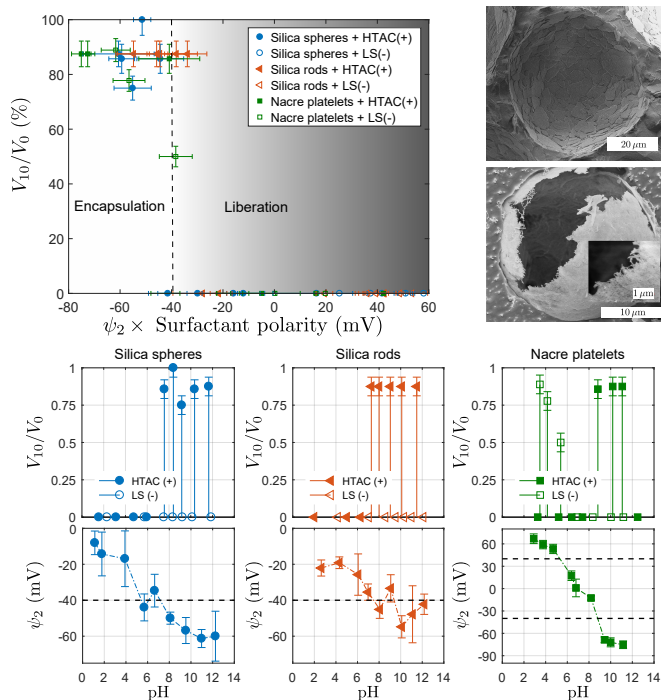


FIG. 2. Graphic representation of the zeta potential criterion for encapsulating and liberating micro-bubbles, formulated with either cationic (HTAC) or anionic surfactants (LS), with different types of particles. The volume of stable micro-bubbles, arbitrarily chosen after 10 days, V_{10} , normalized by the initial volume, V_0 , is plotted against the zeta potential multiplied by the polarity of the ionic surfactant head group. A distinct transition at a zeta potential of ± 40 mV is observed. Once encapsulated the micro-bubbles can be liberated by adjusting the solution pH to lower the zeta potential of the particles. Bottom: Evolution of the normalized volume of encapsulated micro-bubbles, V_{10}/V_0 , and evolution of the zeta potential of the encapsulating particles ψ_2 , both, as a function of the pH of the solution used. Two cryo-SEM images present examples of encapsulated micro-bubbles with 100 nm long boehmite needles, and micrometric nacre platelets.

measurements, by providing a graphic representation of the zeta potential criterion for encapsulating or liberating micro-bubbles with those various particles. We observe a distinct transition at a particle surface potential of around ± 40 mV where encapsulation occurs. It is remarkable that this experimentally determined value for a successful micro-bubble encapsulation is found for all of the various particles studied. However, the zeta potential measurement (using electrophoretic mobility experiments) is indirect and based on a model that considers monodisperse spheres, while some of our samples are highly non-spherical (rods, platelets) and polydisperse. Nevertheless, the robustness of our findings clearly indicates that the double-layer forces play a predominant role in our electrostatic encapsulation process.

We demonstrate the general feature of our encapsulation process, showing that it can also be implemented with silicate precursor anions [32] instead of particles,

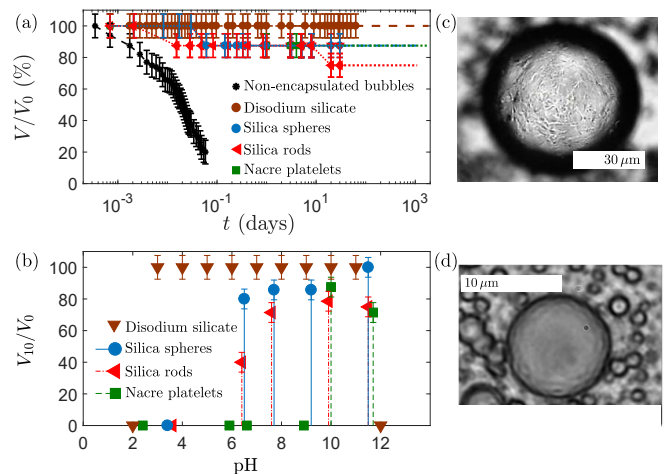


FIG. 3. (a) Temporal evolution of the volume V of micro-bubble dispersions prepared with HTAC cationic surfactants and encapsulated with either silica spheres, rods, nacre platelets or polymerizable precursors (metasilicate anions), normalized by their initial volume V_0 , systematically monitored from one minute up to two months, and directly observed up to five years. (b) A pH-sweep over ten-day-old stable encapsulated micro-bubble dispersions (formulated with HTAC at the CMC) that shows the capsules can be fragmented and gas liberated, by adjusting the pH values of their solution outside their respective encapsulating range, bringing the particle zeta potential below/above ± 40 mV, for which, the global volume of the capsule dispersions drops. Optical microscope images of an air bubble (c) and a dodecane oil droplet (d), both encapsulated by a continuous silicate shell.

and equally applied to liquid droplets. Typical microscopic images of such capsules are shown Fig.3. As with particle encapsulation, we simply mix a sample of dispersed HTAC templated micro-bubbles with an equal volume of 0.1 M disodium metasilicate solution Na_2SiO_3 , adjusted to pH 8.5 prior to use (~ 30 s). Upon addition of acid, this stable alkaline solution (pH > 11) reacts with hydrogen ions to promote silicic acid polymerization, forming a glassy solid. The silicate anions attracted to the cationic surfactant head groups creates a solidified shell around the bubble interface. Unlike alkylsiloxanes, this rapid reaction at room temperature does not create alcoholic by-products. Adjusting the silicate concentration, the shell thickness can be varied. Under our experimental conditions (60 vol% gas-bubble dispersions of around $50 \mu\text{m}$ diameter), at 0.1 M, the mean thickness can be estimated around 35 nm; while below, it is insufficient to completely cover the bubbles' surface. Further increases in disodium metasilicate molarity leads to simultaneous gelation of the excess metasilicate in solution, and even bubbles enclosed within a solid matrix, as shown in *Supplementary Material*.

Once encapsulated our various micro-bubbles, which can be easily re-dispersed in solution, remain unchanged at room temperatures for months and years. Indeed, we demonstrate their extreme long-term stability by showing in Fig. 3(a) the temporal evolution of the volume of differ-

ent dispersions of micro-bubbles originally prepared with a cationic surfactant (HTAC) at CMC, encapsulated with different species (various particles or disodium metasilicate anions), renormalized by their initial volume V_0 , around 25 mL. While the assembly of such micro-bubbles without any encapsulating protective shells shrinks very quickly (on minute time scales) and completely disappears in less than 2 hours, by disproportionation and coalescence, the volume of our various samples of encapsulated micro-bubbles dispersions remains equal to its initial value V_0 or shows only a slight decrease of a few percent after two months. Furthermore, a direct visual inspection of our samples up to five years confirmed that our various encapsulated samples remain strikingly unchanged, showing that our various formulated shells completely prevent and block the microbubbles aging process. Interestingly, we also show in Fig. 3(b) that our electrostatic encapsulation process using particulate materials is reversible: with a pH adjustment bringing the pH values of their solution outside their respective encapsulating range (particle zeta potential below/above $\pm 40\text{mV}$), the particle-based shells capsules can be fragmented, and gas liberated, thus, allowing the controlled release of encapsulated payloads. On the other hand, using polymerizable precursors (silicate anions) as encapsulating species, the subsequent glassy continuous silicate shells are chemically resistant, and the encapsulation is irreversible.

Finally, our encapsulation process can be easily upscaled for industrial developments [5, 6]. It simply requires a step-wise procedure, where a free-flowing ionic surfactant-saturated bubble dispersion is produced first, and then simply mixed with oppositely charged species. An appropriate micro-bubble generation technique, allowing for a free-flowing bubble dispersion (gas volume fraction below 64%) to avoid inter-bubble adhesion with unrestricted access to the bubble surface of encapsulating species is indeed the first crucial step. As such, we have adopted a continuous stirred-tank reactor bubble generation process [33], shown in *Supplemental Material*. Then, our electrostatic encapsulation process simply requires that the number of ionic surfactants adsorbed to the bubble surface is greater than the ones in solution. Such a controlled partitioning ensures that any oppositely charged encapsulating species subsequently added to the gas-bubble dispersion will be attracted to the bubble surface, instead of being neutralized by free surfactants in solution. To determine this condition, we can estimate the adsorption density of surfactant over the particles' surface after microbubble formation by computing the ratio between the surfactant available in solution to the available particle surface area, $r = (N_S - N_{Sb})/N_p A_p$, with N_S the total number of surfactants, N_{Sb} the number of surfactants adsorbed to the bubble surface upon mi-

crobubble formation, A_p the surface area of the particle considered, and N_p the number of particles. We could estimate this ratio r for spherical silica particles of various size in HTAC surfactant solutions at different concentrations used to generate 50 μm bubbles. A successful encapsulation occurs when $r \leq 0.75$ molecules/ nm^2 (see *Supplementary Material*). Such a result is in quantitative agreement with the measurement of Tyrode et al [4], who could show that silica particles are not completely covered by the surfactants for such adsorption density values. Then, the oppositely charged particles can be attracted and attached to the bubble surface. If we exceed this coverage (increasing for instance the surfactant concentration), the particles will become partially hydrophobic, create hemimicelles [4] and aggregate to form flocs in solution, which subsequently prevents their attraction to the charged bubbles. Therefore, our encapsulation method is not due to an in-situ modification of the particles' wettability: in contrast to the "Pickering" technique, we use hydrophilic particles.

To conclude, this Letter presents an original method for producing micro-capsules. The "Pickering" stabilization of foams and emulsions with hydrophobic particles has been used for decades. However, the hydrophobic particle interaction with the surface of bubbles or droplets is still not clearly understood, and carrying out such a technique at an industrial scale is difficult. In stark contrast, our novel approach, which can be quantitatively described with DLVO theory, circumvents these difficulties. Therefore, we reveal a new way to guide self-assembly with electrostatics as the driving force, allowing the formulation of novel objects, stable for years, at low cost and at industrial levels, thanks to the creation of a diverse variety of protective shells. Indeed, our general and simple electrostatic encapsulation process can also be implemented with polymerizable precursor anions instead of particles, and applied to liquid droplets, thus, paving the way to the formulation of more elaborate macroscopic structures. For instance, the use of metallic particles [35] can lead to the development of switchable photonic fluids, with plasmonic capsules [36] and liquid mirrors [37].

We thank S. Parola and F. Chaput for providing tailor-made nano-needles, D. Chateau, E. Freyssingas, C. Place, S. Parola, A. Asnacios, J.-T. Simonnet, A. Lafuma, F. Levy, for fruitful discussions and access to various equipments in their laboratories. V.B. wishes to dedicate this work to UC Berkeley Professors Clayton Radke and Douglas Fuerstenau, and the deceased Professors Felix Sebba and Pierre-Gilles de Gennes.

This work was partially funded by L'Oreal, and ANR Tremplin ERC "PhoFo".

[1] J. Rodriguez-Rodriguez, A. Sevilla, C. Martinez-Bazan, J. M. Gordillo, Generation of microbubbles with applica-

tions to industry and medicine. Annual Review of Fluid

- Mechanics 47, 405-429 (2015).
- [2] M. Versluis, E. Stride, G. Lajoinie, B. Dollet and T. Segers Ultrasound Contrast Agent Modeling: A Review, *Ultrasound in Medicine and Biology* Volume 46, Issue 9, September Pages 2117-2144 (2020).
 - [3] Y. Liu, H. Miyoshi, M. Nakamura, Encapsulated ultrasound microbubbles: therapeutic application in drug/gene delivery. *Journal of controlled release* 114 (1), 89-99 (2006).
 - [4] A. Agarwal, W. J. Ng, Y. Liu, Principle and applications of microbubble and nanobubble technology for water treatment. *Chemosphere* 84 (9), 1175-1180 (2011).
 - [5] V. Bergeron, J. T. Simonnet, F. Levy, A. Lafuma, S. Santucci, inventors; L'Oreal SA, assignee, Bubble encapsulation via silicic acid complexation. US patent 9,452,406 B2, September 27 (2016).
 - [6] V. Bergeron, J. T. Simonnet, F. Levy, A. Lafuma, S. Santucci, inventors; L'Oreal SA, assignee, Stable bubbles via particle absorption by electrostatic interaction. US patent 9,433,578 B2, September 6 (2016).
 - [7] F. L. Tchienbou-Magaia, I. T. Norton, P. W. Cox, Microbubbles with protein coats for healthy food: Air filled emulsions in Gums and Stabilisers for the Food Industry 15 (The Royal Society of Chemistry, 2009), pp. 113-125.
 - [8] C. E. P. Epstein, M. S. Plesset, On the stability of gas bubbles in liquid gas solutions. *Journal of Chemical Physics* 18 (11), 1505-1509 (1950).
 - [9] M. M. Lozano, M. L. Longo, Microbubbles coated with disaturated lipids and DSPE-PEG2000: phase behavior, collapse transitions, and permeability. *Langmuir* 25 (6), 3705-3712 (2009).
 - [10] E. Talu, M. M. Lozano, R. L. Powell, P. A. Dayton, M. L. Longo, Long-term stability by lipid coating monodisperse microbubbles formed by a flow-focusing device. *Langmuir* 22 (23), 9487-9490 (2006).
 - [11] F. Caruso, R. A. Caruso, H. Mohwald, Nanoengineering of inorganic and hybrid hollow spheres by colloidal templating. *Science*, 282 (5391), 1111-1114 (1998).
 - [12] O. D. Velev, K. Furusawa, K. Nagayama, Assembly of latex particles by using emulsion droplets as templates. 1. Microstructured hollow spheres. *Langmuir* 12 (10), 2374-2384 (1996).
 - [13] A. D. Dinsmore, M.F. Hsu, M. G. Nikolaides, M. Marquez, A. R. Bausch, D. A. Weitz, Colloidosomes: selectively permeable capsules composed of colloidal particles. *Science* 298 (5595), 1006-1009 (2002).
 - [14] R. K. Rana, Y. Mastai, A. Gedanken, Acoustic cavitation leading to the morphosynthesis of mesoporous silica vesicles. *Advanced Materials* 14 (19), 1414-1418 (2002).
 - [15] C. J. Everson, Process of Concentrated Ores. US Patent 348,157 A, August 24 (1886).
 - [16] W. Ramsden, Separation of solids in the surface-layers of solutions and suspensions (observations on surface-membranes, bubbles, emulsions, and mechanical coagulation). Preliminary account. *Proceedings of the royal Society of London* 72 (477-486), 156-164 (1904).
 - [17] S. U. Pickering, CXCVI-Emulsions. *Journal of the Chemical Society, Transactions* 91, 2001-2021 (1907).
 - [18] B. Binks and R. Murakami, Phase inversion of particle-stabilized materials from foams to dry water, *Nature Materials*, 5, 865, (2006).
 - [19] A. Cervantes Martinez, E. Rio, G. Delon, A. Saint-Jalmes, D. Langevin and B. P. Binks, On the origin of the remarkable stability of aqueous foams stabilised by nanoparticles: link with microscopic surface properties, *Soft Matter*, 4, 15311535, (2008).
 - [20] N. Taccoen, F. Lequeux, D. Z. Gunes, and C. N. Baroud, Probing the Mechanical Strength of an Armored Bubble and Its Implication to Particle-Stabilized Foams, *Phys. Rev. X* 6, 011010 (2016).
 - [21] E. Dickinson, Food emulsions and foams: stabilization by particles. *Current Opinion in Colloid and Interface Science* 15 (1), 40-49 (2010).
 - [22] P. Finkle, H. D. Draper, J. H. Hildebrand, The theory of emulsification. *Journal of the American Chemical Society* 45 (12), 2780-2788 (1923)
 - [23] A. F. Koretsky, P. M. I. Kruglyakov, Emulsifying effects of solid particles and the energetics of putting them at the wateroil interface. *Izv. Sib. Otd. Akad. Nauk SSSR, Ser. Khim. Nauk* 2, 139 (1971).
 - [24] J. Ralston, D. Fornasiero, N. Mishchuk, The hydrophobic force in flotation-a critique. *Colloids and Surfaces A: Physicochemical and Engineering Aspects* 192 (1), 39-51 (2001).
 - [25] Y. Xing, X. Gui, Y. Cao, The hydrophobic force for bubble-particle attachment in flotation, *Physical Chemistry Chemical Physics* 19 (36), 24421-24435 (2017).
 - [26] J. N. Israelachvili, *Intermolecular and surface forces* (Academic press, 2011).
 - [27] R. Hogg, T. W. Healy, D. W. Fuerstenau, Mutual coagulation of colloidal dispersions. *Transactions of the Faraday Society* 62, 1638-1651 (1966).
 - [28] S. Usui, H. Sasaki, Zeta potential measurements of bubbles in aqueous surfactant solutions. *Journal of Colloid and Interface Science* 65 (1), 36-45 (1978).
 - [29] R. F. Tabor, R. Manica, D. Y. C. Chan, F. Grieser and R. R. Dagastine, Repulsive van der Waals forces in soft matter: why bubbles do not stick to walls, *Phys. Rev. Lett.*, 2011, 106, 064501.
 - [30] M. Bostrom, D. R. M. Williams, and B. W. Ninham, Specific ion effects: why DLVO theory fails for biology and colloid systems. *Physical Review Letters*, 87(16), 168103.
 - [31] D.W. Fuerstenau, A century of developments in the chemistry of flotation processing in Froth flotation: a century of innovation, M. C. Fuerstenau, G. J. Jameson, R. H. Yoon, Eds. (SME, 2007), pp 3-64.
 - [32] K. J. Edler, Soap and sand: construction tools for nanotechnology, *Phil. Trans. R. Soc. Lond. A* (2004) 362, 2635-2651
 - [33] F. Sebba, An improved generator for micron-sized bubbles. *Chemistry and Industry* 3, 91-92 (1985).
 - [34] E. Tyrode, M.W. Rutland and C. D. Bain, Adsorption of CTAB on Hydrophilic Silica Studied by Linear and Nonlinear Optical Spectroscopy, *Journal of the American Chemical Society*, 130, 1743417445 (2008).
 - [35] D. Chateau, A. Desert, F. Lerouge, G. Landaburu, S. Santucci, S. Parola, Beyond the Concentration Limitation in the Synthesis of Nanobipyramids and Other Pentatwinned Gold Nanostructures, *Appl. Mater. Interfaces*, 11, 42, 39068-39076 (2019)
 - [36] C. Burel, A. AlSayed, L. Malassis, C.B. Murray, B. Donnio and R. Dreyfus Plasmonic-based mechanochromic microcapsules as strain Sensors, *Small*, 13, 1701925 (2017)
 - [37] Y. Montelongo, D. Sikdar, Y. Ma, A. J. S. McIntosh, L. Velleman, A. R. Kucernak, J. B. Edel and A. Kornyshev Electrotunable nanoplasmonic liquid mirror. *Nature Materials*, 16, 11271135 (2017)

Supplemental Material

I. BUBBLE GENERATION PROCESS

An appropriate micro-bubble generation technique is a first crucial step for our encapsulation method. Therefore, we implemented a continuous stirred-tank reactor bubble generation process, originally developed by Sebba [1], for creating, at low-cost, industrial quantities of micro-bubbles, in the size range of 10 - 200 μm diameter, with a mean bubble diameter around 50 μm [1, 2].

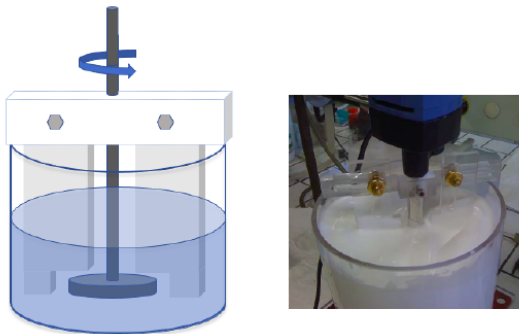


FIG. 1. A disc agitator (70 mm diameter, 5 mm thickness) spinning at a speed of 10 000 rpm between two stationary baffles stirs within a 3 L plastic beaker, 1 L of a surfactant solution at the critical micellar concentration (CMC), to create a free flowing 60 vol% air dispersion of micro-bubbles.

Our reactor is shown in Figure S1; it consists of a 3 L plastic beaker equipped with a central stainless-steel disc agitator spinning between two stationary baffles. Stirring 1 L of a surfactant solution at the critical micellar concentration (CMC) to a disc speed of 10 000 rpm produces large-scale quantities of a free flowing 60 vol% air dispersion of micro-bubbles.

II. ELECTROSTATIC ENCAPSULATION

Once such micro-bubbles dispersion is produced, we then simply mix samples of equal volumes (typically 25 mL) of these dispersed micro-bubbles with a solution of properly chosen (pH adjusted) oppositely charged particles or polymeric precursors.

To encapsulate those micro-bubbles with particle-based shells, we use typically 25 mL solution of particles at 5 wt%, in pH adjusted pure water. As explained and shown in the manuscript, to demonstrate the robustness of our novel encapsulation method, we have performed experiments with a variety of particles of different shapes (spheres, rods, needles, platelets), bulk materials (silica, boehmite, nacre), and either cationic (Hexadecyl Trimethyl Ammonium Chloride, (HTAC)), or anionic (Lauroyl Sarcosinate (LS)) surfactant solutions.

On the other hand, to formulate continuous silicate shells, we mix a sample of dispersed HTAC templated micro-bubbles with an equal volume of disodium metasilicate solution Na_2SiO_3 , adjusted to pH 8.5 prior to use (~ 30 s) to trigger a silicic acid polymerization.



FIG. 2. Typical 10 hours-old samples of dispersions of air micro-bubbles encapsulated with a silicate shell. Those samples were obtained by mixing equal volumes (25 mL) of dispersed HTAC stabilized micro-bubbles with a disodium metasilicate solution (pH adjusted to trigger the silicic acid polymerization). We show the impact of the concentration of disodium silicate, at 0.18 M (#1bis) and 0.09 M (#2). Without any encapsulating protective shells (sample (#0)), the micro-bubbles dispersions disappears in less than 2 hours.

We could observe the impact of the concentration of disodium metasilicate on the encapsulated micro-bubbles dispersions. Figure S2 displays two different samples of 10 hours-old encapsulated micro-bubbles obtained at 0.18 M (#1bis) and 0.09 M (#2). When the silicate concentration is larger than 0.1 M the volume of our samples of encapsulated micro-bubbles dispersions remains unchanged (or slightly decreases by a few percent) over a period of one month, while below, it is insufficient to completely cover the bubbles' surface. On the other hand, further increases in disodium metasilicate molarity leads to simultaneous gelation of the excess metasilicate in solution, and even bubbles enclosed within a solid matrix. As one can notice in the sample #1bis at 0.18 M, the drained solution forms a gel and becomes slightly opaque due to excess disodium silicate in solution.

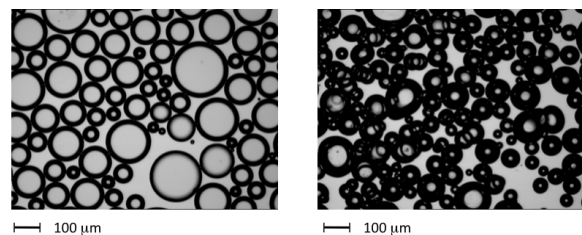


FIG. 3. (Left) Optical microscope image of air bubbles dispersion (few minutes old), obtained with our continuous stirred-tank reactor, using a cationic (HTAC) surfactant solution at the CMC ($\approx 10^{-3}\text{M}$). (Right) Optical microscope image of the same dispersion of air bubble, encapsulated with a silicate shell, obtained after mixing equal volumes of the dispersed HTAC stabilized micro-bubbles with a (pH adjusted) disodium metasilicate solution at 0.1 M.

We also provide in Figure S3 microscope images of the air micro-bubble dispersion, generated thanks to our continuous stirred-tank reactor, as well as those bubbles encapsulated with a continuous silicate shell, using a Na_2SiO_3 solution at 0.1 M, both few minutes old. One can directly notice the size difference between the bubbles and the capsules, related to the quick bubbles coarsening, while collecting them with a syringe on the microscope slides. Indeed, without any any encapsulating protective shells, the micro-bubbles shrink very quickly and completely disappears in less than 2 hours, by disproportionation and coalescence, as shown in the corresponding video Movie.1.avi, where 360 images were recorded during 1 hour (at a rate of 1 frame every 10 seconds), as well as on the macroscopic sample displayed Figure S2 (sample (#0)). In stark contrast, our various formulated shells completely prevent and block the micro-bubbles aging process, as shown both on the microscopic image Fig. S3 (Right) and the corresponding video Movie.2.avi, where we recorded 200 images at the same rate of 1 frame every 10 seconds, as well as on the macroscopic (few hours-old) samples, displayed Figure S2 (sample (#1bis and #2)).

III. ADSORPTION DENSITY OF SURFACTANTS OVER THE PARTICLES' SURFACE

It is important to understand how the surfactant concentration and particle size influence the encapsulation process. If excessive surfactant remains in solution after microbubble formation it can adhere to the particles and neutralize them. To determine this condition, we can estimate the adsorption density of surfactant over the particles' surface after microbubble formation by computing the ratio between the surfactant available in solution, to the available particle surface area, $r = \frac{N_S - N_{Sb}}{N_p A_p}$, with N_S the total number of surfactants, N_{Sb} the number of surfactants adsorbed to the bubble surface upon microbubble formation, A_p the surface area of the particle

considered, N_p the number of particles.

We have estimated the adsorption density of cationic HTAC surfactant over the surface of spherical silica particles of various diameters D (40 nm, 100 nm and 255 nm), after the creation of micro-bubbles (60 vol% gas-bubble dispersions of around 50 μm diameter) at different surfactants concentrations, 1, 10 and 100 times the critical micelle concentration (CMC $\simeq 10^{-3}\text{M}$). The surfactant air/water adsorption is 46 $\text{A}^2/\text{molecule}$ [3] and the particle concentration of 5 wt%. The table I provides the corresponding values of this adsorption density r in molecules/ nm^2 . We observe a successful encapsulation, when the ratio between the surfactant available in solution after the formulation of the air bubble dispersion and the available particle surface area has a value smaller than 0.75 molecules/ nm^2 . As shown by Tyrode et al [4], for a similar surfactant (CTAB) adsorbed to silica particles, for such values of this adsorption density, one can consider that the particles are not completely covered by the surfactants, and thus their surface potential will not be completely neutralized.

	Particle Size		
[HTAC]	40 nm	100 nm	255 nm
1 CMC	0.05	0.13	0.3
10 CMC	0.7	2	5
100 CMC	8	20	50

TABLE I. Adsorption density r (molecules/ nm^2) of surfactants at the particles' surface, for different solutions of spherical silica particles and microbubbles dispersions obtained with cationic (HTAC) surfactant at different concentrations (1, 10 and 100 times the critical micelle concentration (CMC $\simeq 10^{-3}\text{M}$) before encapsulation). A successful encapsulation is observed when this adsorption density is lower than 0.75 molecules/ nm^2 . The corresponding values for which encapsulation is possible are highlighted in bold.

- [1] F. Sebba, An improved generator for micron-sized bubbles. *Chemistry and Industry* 3, 91-92 (1985).
 [2] D. L. Michelsen, F. Sebba, "Microbubble Generator", US Patent 5, 314, 644 A, May 24 (1994).
 [3] V. Bergeron, Disjoining pressures and film stability of alkyltrimethylammonium bromide foam films. *Langmuir*,

- 13(13), 3474-3482 (1997).
 [4] E. Tyrode, M.W. Rutland and C. D. Bain, Adsorption of CTAB on Hydrophilic Silica Studied by Linear and Nonlinear Optical Spectroscopy, *Journal of the American Chemical Society*, 130, 17434-17445 (2008).